International Journal of Rotating Machinery
1995, Vol. 2, No. 2, pp. 123-129
Reprints available directly from the publisher
Photocopying permitted by license only

© 1995 OPA (Overseas Publishers Association)
Amsterdam B.V. Published in The Netherlands
by Harwood Academic Publishers GmbH
Printed in Singapore

A Numerical Analysis on Flow and Heat Transfer in the Entrance Region of an Axially Rotating Pipe

SHUICHI TORII
Department of Mechanical Engineering, Kagoshima University, 1-21-40 Korimoto, Kagoshima 890, Japan

WEN-JEI YANG
Department of Mechanical Engineering and Applied Mechanics, The University of Michigan, Ann Arbor, Michigan, 48109, U.S.A.

A numerical study is performed to investigate turbulent flow and heat transfer characteristics in the entrance region of a pipe rotating around its axis. Various different k-ϵ turbulence models are employed whose function consists of the Richardson number in the ϵ model to take swirling into account. The axial rotation of the pipe suppresses thermal development and causes a substantial decrease in the Nusselt number along the flow. It is disclosed from the study that an increase in the rotation rate induces a reduction in the velocity gradient, turbulent kinetic energy and Reynolds stress in the vicinity of the wall and a substantial deformation of these radial profiles in the downstream direction. It results in both a suppression of the thermal development and an attenuation in the Nusselt number along the flow.

Key Words: Numerical analysis; swirling flow; turbulent flow; pipe flow; heat transfer

INTRODUCTION

Transport phenomena in a pipe rotating around its axis are encountered in many industrial applications such as flows in the inlet part of fluid machinery, rotating heat exchangers and cooling systems of rotors. There was many numerical and experimental investigations on this subject, but only a few will be cited below, which are pertinent to the present study.

Murakami and Kikuyama [1980] conducted an experimental study on the velocity profile and hydraulic loss in a saturated downstream region of a rotating pipe. It was disclosed that both turbulence and hydraulic loss were remarkably reduced due to pipe rotation and that streamwise velocity profile gradually deformed into a parabolic form with an increase in its speed. Kikuyama et al. [1983] determined the variation of streamwise velocity profiles using a modified mixing length theory proposed by Bradshaw [1969]. The same numerical analysis was performed by Hirai et al. [1986] using the Reynolds stress model. It was found that a change in flow characteristics induced by a swirl could be attributed to a decrease in the Reynolds stress. A combined experimental and theoretical study was performed to determine the effects of pipe rotation on fluid flow and heat transfer in a thermally and hydrodynamically fully developed flow region [1988]. It was found that an increase in the rotation rate resulted in a decrease in heat transfer performance with the Nusselt number asymptotically approaching that of a laminar pipe flow. Torii and Yang [1994] modified the existing k-ϵ turbulence models to increase swirling effects. In their model, a function including the Richardson numbers was proposed and introduced into the ϵ equation. The model yields substantial decreases in the friction coefficient, turbulent kinetic energy, Reynolds stress and streamwise velocity gradient in the vicinity of the wall.

Nishibori et al. [1987] investigated the transport phenomena in the entrance region of an axially rotating pipe. The boundary layer was found to be strongly stabilized by the centrifugal force due to the rotating velocity component, resulting in a laminarization of the flow. Weigrand and Beer [1990] investigated fluid flow and heat transfer characteristics in a combined hydrodynamic and thermal entrance region using a modified mixing length hypothesis, which takes into account turbulence

suppression due to the centrifugal force. It was disclosed that the entrance length increases significantly with an increase in the rotation rate. However, flow laminarization mechanisms in the entrance region, particularly changes in the flow structures due to pipe rotation, are not clearly understood.

The purpose of the present study is to investigate transport phenomena in a hydorodynamically-and-thermally-developing flow region of an axially rotating pipe with uniform heat flux. Emphasis is placed on the effects of pipe rotation on flow structures and heat transfer rate. Numerical results obtained by using the existing k-ϵ turbulence models are compared.

THEORETICAL ANALYSIS

Governing Equations

A steady flow through a slightly heated circular pipe rotating around its axis is treated, in which the boundary layer is developing both thermally and hydrodynamically. The physical configuration and the cylindrical coordinate system are shown in Fig. 1. The following assumptions are imposed in the formulation of the problem: incompressible, turbulent, steady flow: constant fluid properties; and negligible axial conduction (in a flow with a high Peclet number). An order-of-magnitude analysis indicates all second-derivative terms to be negligible in the streamwise direction. The simplified governing equations read as follows:

Continuity equation:

$$\frac{\partial u}{\partial x} + \frac{\partial v}{\partial r} + \frac{v}{r} = 0 \tag{1}$$

Momentum equations:

x direction:

$$u\frac{\partial \bar{u}}{\partial x} + v\frac{\partial \bar{u}}{\partial r} = -\frac{1}{\rho}\frac{d\bar{P}}{dx} + \frac{1}{r}\frac{\partial}{\partial r}(r\nu\frac{\partial \bar{u}}{\partial r} - ru'v') \tag{2}$$

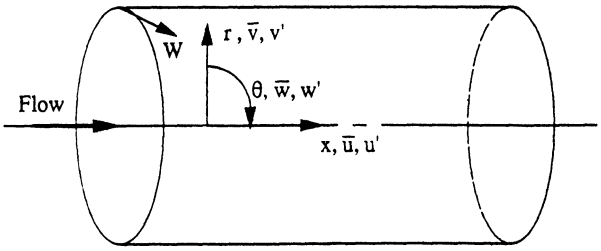

FIGURE 1 Coordinate system.

r direction:

$$\frac{\bar{w}^2}{r} = \frac{1}{\rho}\frac{\partial \bar{P}}{\partial r} \tag{3}$$

θ direction:

$$u\frac{\partial \bar{w}}{\partial x} + v\frac{\partial \bar{w}}{\partial r} = \frac{\overline{vw}}{r} = \frac{1}{2\partial r}\{r^3\nu\frac{\partial(\frac{w}{r})}{\partial r} - r^2\frac{r}{v'w'}\} \tag{4}$$

Energy equation:

$$u\frac{\partial \bar{T}}{\partial x} + v\frac{\partial \bar{T}}{\partial r} = \frac{1}{r\partial r}(r\alpha\frac{\partial \bar{T}}{\partial r} - \overline{rv't'}) \tag{5}$$

The Boussinesq's approximation yields, the Reynolds stresses $\overline{-u'v'}$ and $\overline{-v'w'}$ in Eqs. (2) and (4) as

$$\overline{-u'v'} = \nu_t\frac{\partial \bar{u}}{\partial r} \text{ and } \overline{-v'w'} = \nu_t r\frac{\partial(\frac{\bar{w}}{r})}{\partial r} \tag{6}$$

and the turbulent heat flux $\overline{-v't'}$ in Eq. (5) as

$$\overline{-v't'} = \alpha_t\frac{\partial \bar{T}}{\partial r} \tag{7}$$

The turbulent viscosity ν_t in Eq. (6) is related to the turbulent kinetic energy k and its dissipation rate ϵ through Kolmogorov-Prandtl's relation [1982], as

$$\nu_t = C_\mu f_\mu\frac{k^2}{\varepsilon} \tag{8}$$

The turbulent thermal diffusivity α_t in Eq. (7) is given by

$$\alpha_t = \frac{\nu_t}{Pr_t} \tag{9}$$

where 0.9 is adopted as the value of Pr_t. In order to evaluate k and ϵ in Eq. (8), a low Reynolds number version of a k-ϵ turbulence model is used in the present study. The transport equations of k and ϵ are

$$u\frac{\partial k}{\partial x} + v\frac{\partial k}{\partial r} = \frac{1}{r\partial r}\{r(\frac{\nu_t}{\sigma_k} + \nu)\frac{\partial k}{\partial r}\} + \nu_t[(\frac{\partial \bar{u}}{\partial r})^2 + \{r\frac{\partial}{\partial r}(\frac{\bar{w}}{r})\}^2] - \epsilon + D \tag{10}$$

$$\bar{u}\frac{\partial \epsilon}{\partial x} + \bar{v}\frac{\partial \epsilon}{\partial r} = \frac{1}{r}\frac{\partial}{\partial r}\{r(\frac{\nu_t}{\sigma_\epsilon} + \nu)\frac{\partial \epsilon}{\partial r}\}$$
$$+C_1 f_1 \frac{\epsilon}{k}\nu_t[(\frac{\partial \bar{u}}{\partial r})^2 + \{r\frac{\partial}{\partial r}(\frac{\bar{w}}{r})\}^2] - C_2 C_3 f_2 \frac{\epsilon^2}{k} + E \quad (11)$$

The k-ϵ models proposed by Launder and Sharma [1974], Nagano and Hishida [1987], and Torii et al. [1990] are employed in the present study. In order to include swirling effect, the model function, C_3 (in Eq. 11)), proposed by Torii and Yang [1994]

$$C_3 = 1 - 0.06\mathrm{Ri}^{0.5}, \quad (12)$$

is employed where

$$\mathrm{Ri} = \frac{k^2\bar{w}\partial(rw)}{\varepsilon^2 r^2 \partial r} \quad (13)$$

The empirical constants and model functions in Eqs. (8), (10) and (11) are summarized in Table 1 for the three turbulence models.

As pointed out by Kawamura and Mishima [1991] and Torii and Yang [1994], if m the approximation of $-v'w'$ in Eq. (6), is employed, the radial profile of the tangential velocity would become linear, and consequently turbulence suppression due to the centrifugal force of a swirling flow would not take place. Weigand and Beer [1990] measured the radial profiles of the time-averaged tangential velocity at different axial locations and derived the universal tangential profiles as

$$w = \mathrm{W}(\frac{r}{d/2})^{(2 + f(z^*))} \quad (14)$$

where

$$f(z^*) = \frac{1}{z^*} + 9.5e^{-0.019z^*} \quad (15)$$

In the present study, Eq. (14) is employed to replace Eq. (14) in determining the tangential velocity equation.

A hydrodynamically, fully-developed isothermal turbulent flow in the absence of rotation is assumed as the inlet condition. Only one-half of the pipe cross section is treated because of a symmetry in the fluid flow. Thus, the boundary conditions are specified as

r = 0 (center line):

$$\frac{\partial \bar{u}}{\partial r} = \frac{\partial \bar{w}}{\partial r} = \frac{\partial k}{\partial r} = \frac{\partial \epsilon}{\partial r} = \frac{\partial \bar{T}}{\partial r} = 0$$

r = d/2 (wall):

$$\bar{u} = \bar{v} = k = \epsilon = 0, \ \bar{w} = \mathrm{W(tangentialvelocity)},$$
$$-\frac{\partial T}{\partial r} = \frac{q_w}{\lambda_w}\,\mathrm{(constantheatflux)}$$

The ranges of the parameters in the present study are: Reynolds numbers Re = 5,000 and 10,000, Prandtl

TABLE 1
Empirical constants and model functions

	Launder & Sharma	Nagano & Hishida	Torii et al.
C_μ	0.09	0.09	0.09
C_1	1.45	1.45	1.44
C_2	2.0	1.9	1.9
C_3	1.0	1.0	1.0
σ_k	1.0	1.0	1.0
σ_ϵ	1.3	1.3	1.3
f_1	1.0	1.0	$1 + 0.15exp(-\frac{R_t}{25})$
f_2	$1 - 0.3exp(-R_t^2)$	$1 - 0.3exp(-R_t^2)$	$1 - 0.3exp(-R_t^2)$
f_μ	$exp\{\frac{-3.4}{(1 - R_t/50)^2}\}$	$\{1 - exp(\frac{R_\tau}{26.5})\}^2$	$\{1 - exp(\frac{R_\tau}{26.5})\}^2$
D	$-2\nu(\frac{\partial\sqrt{k}}{\partial r})^2$	$-2\nu(\frac{\partial\sqrt{k}}{\partial r})^2$	$-2\nu(\frac{\partial\sqrt{k}}{\partial r})^2$
E	$2\nu\nu_t(\frac{\partial^2\bar{u}}{\partial r^2})^2$	$\nu\nu_t(1 - f_\mu)(\frac{\partial^2\bar{u}}{\partial r^2})^2$	$\nu\nu_t(1 - f_\mu)(\frac{\partial^2\bar{u}}{\partial r^2})^2$

number Pr = 0.7 (air) and rotation rates N = 0, 1, 2 and 3.

Numerical Method

The governing equations employed are discretized using a control volume finite difference procedure [1980]. Since all turbulence quantities as well as the time-averaged axial and tangential velocities vary rapidly in the near-wall region, two control volumes are always located within the viscous sublayer, $y^+_* = 5$. The radial mesh size is increased from a minimum value adjacent to the wall towards the center line in geometrical proportion, and the maximum control volume size near the center line is always kept within 3% of d/2. Meanwhile, the axial control volume size is constant at five times the minimum radial size for the wall. Since the governing equations are essentially parabolic, calculation is performed from the inlet in the downstream direction by means of the marching procedure. At each axial location, the axial pressure gradient $d\bar{P}/dx$ is assumed and the procedure is repeated until the criterion of convergence is satisfied, which is set at

$$\max \left| \frac{\phi^M - \phi^{M-1}}{\phi M-1} \right| < 10^{-4} \qquad (16)$$

for all the variables ϕ ($\bar{u}$, $\bar{v}$, $\bar{T}$, k, and ϵ). The superscripts M and M − 1 in Eq. (16) indicate two successive iterations, while the subscript "max" refers to a maximum value over the entire fields of iterations. Since the streamwise velocity obtained must satisfy the continue equation, the axial pressure gradient is corrected and the computation is repeated for a new axial velocity, until the total mass flow rate is satisfied under the criterion:

$$\frac{\int\int \bar{u}_{cp} d\theta dr - \int\int u_{in} d\theta dr}{\int\int \bar{u}_{in} d\theta dr} \leq 10^{-5} \qquad (17)$$

where $\bar{u}_{cp}$ is the axis velocity under the correction process.

Throughout numerical calculations, the number of control volumes in the radial direction was properly selected between 51 and 78 to ensure validation of the numerical procedures as well as to obtain grid-independent solutions. The maximum relative error over all dependent variables within this change of grid spacing was kept within 1%. The computations are processed in the following order:

1. Specify the initial values of $\bar{u}$, $\bar{v}$, $\bar{w}$, $\bar{T}$, k, and ϵ, and assign a constant axial pressure gradient.
2. Solve the equations of $\bar{u}$, $\bar{v}$, $\bar{T}$, k, ϵ, and Eq. (14) for $\bar{w}$.
3. Repeat step 2 until the criterion of convergence, Eq. (16), is satisfied for all dependent variables.
4. Calculate new values of $\bar{u}$, $\bar{v}$, $\bar{w}$, $\bar{T}$, k, and ϵ with a corrected new axial pressure gradient.
5. Repeat steps 2–4 until the conservation of the streamwise flow rate is satisfied under the criterion, i.e. Eq. (17), followed by evaluating convergent values of $\bar{u}$, $\bar{v}$, $\bar{w}$, $\bar{T}$, k, and ϵ.
6. Repeat step 2–5 until x reaches the designated length.

The CPU time required in computing this scheme was about 24 to 100 hours on a NEC personal computer (32 bit), depending on the number of control volumes used.

RESULTS AND DISCUSSION

Numerical results for the Nusselt number Nu are illustrated in Figs. 2, 3 and 4 in the form of Nu/Nu_o versus x/d, with N as the parameter, for the k-ϵ models of Launder and Sharma [1974], Nagano and Hishida [1987], and Torii et al. [1990], respectively. Here, Nu_o denotes Nu for a fully-developed turbulent pipe flow without rotation. The cases (a) and (b) in each figure correspond to Re = 5,000 and 10,000 respectively. The Nusselt number decreases monotonically along the flow due to the thermal entrance effect, and approaches an asymptotic value. It is observed that for a given Re, an

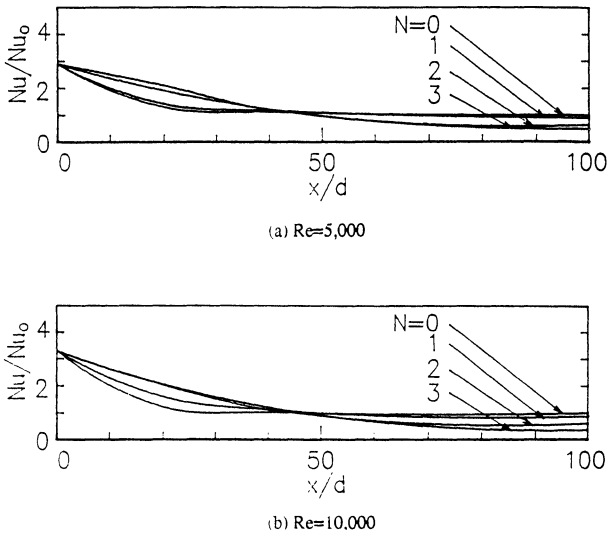

FIGURE 2 Local Nusselt number using the k − ϵ model of Launder and Sharma [1974], at (a) Re = 5,000 and (b) 10,000.

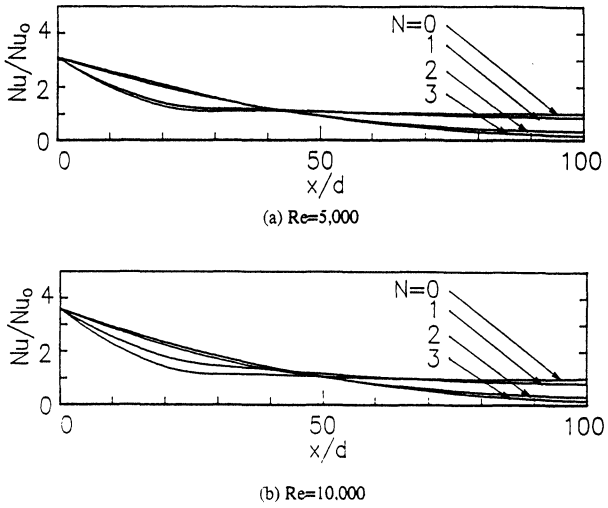

FIGURE 3 Local Nusselt number using the k − ϵ model of Nagano and Hishida [1987], at (a) Re = 5,000 and (b) 10,000.

increase in N suppresses a thermal development and induces an attenuation in the Nusselt number, whose asymptotic value is attained in the downstream region. The same tendency is observed at different Reynolds numbers. In all three models, the thermal entrance region is further extended with an increase in the rotational speed of the pipe. An examination of Figs. 2, 3 and 4 discloses the extent of effects of N on Nu.

Next is to explore the mechanism of turbulent transport phenomena using the k-ϵ model of Torii et al. [1990], at N = 1 and 3, Re = 10,000. The radial profiles of the time-averaged streamwise velocity, $\bar{u}/U$, at different axial locations are illustrated in Fig. 5, in which the

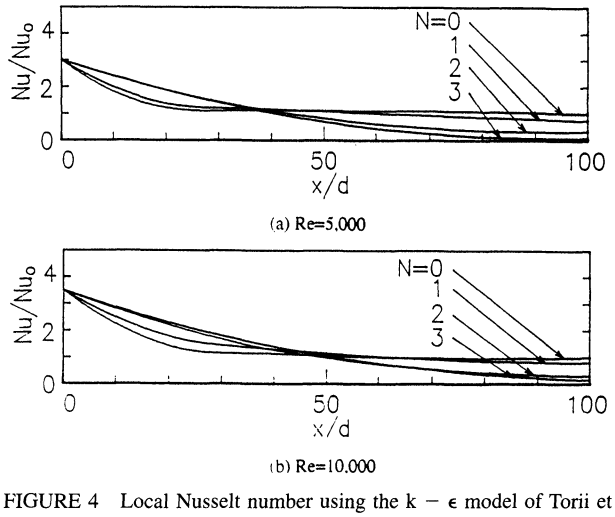

FIGURE 4 Local Nusselt number using the k − ϵ model of Torii et al. [1990], at (a) Re = 5,000 and (b) 10,000.

experimental data of Nishibori et al. [1987] are superimposed for comparison. The cases (a) and (b) in Fig. 5 correspond to N = 1 and 3, respectively. Although a slight change in recognized in the velocity gradient at the wall, a nearly similar shape is seen to be maintained along the flow, resulting in a slight deformation of the velocity distribution due to the pipe rotation, as shown in Fig. 5(a). In contrast, a remarkable change in its shape is seen in the case of a higher rotation speed, Fig. 5(b). It is seen that as the flow goes downstream, the streamwise

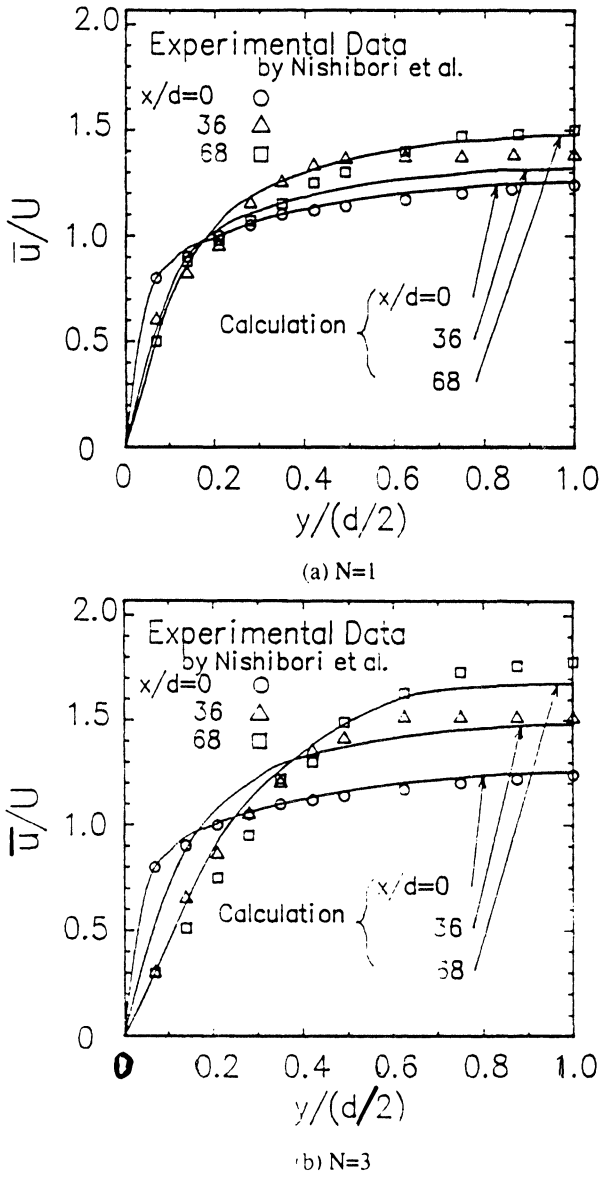

FIGURE 5 A comparison of predicted velocity profiles with existing experimental data for Re = 10,000 at different axial locations, using the k − ϵ model of Torii et al. [1990], at (a) N = 1 and (b) N = 3.

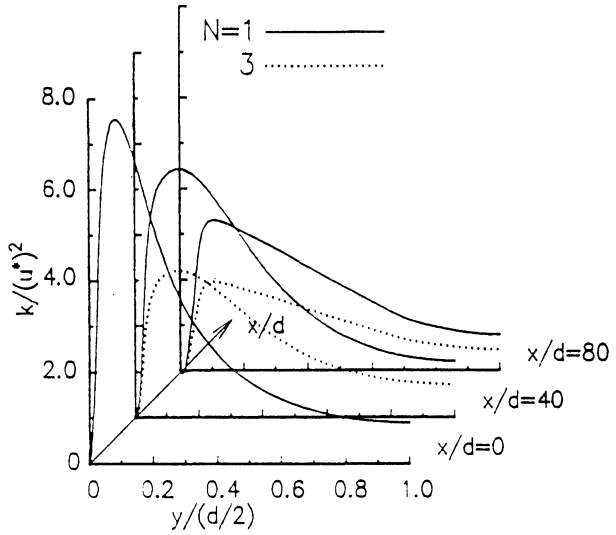

FIGURE 6 Streamwise variation of turbulent kinetic energy profiles, using the k − ϵ model of Torii et al. [1990], for Re = 10,000.

velocity profile gradually forms a parabolic curve, indicating a reverse transition from turbulent to laminar flow. Figure 6 illustrates the streamwise variation of the radial profiles of turbulent kinetic energy, which is normalized by the square of the friction velocity, u*, for a stationary pipe flow. The turbulent kinetic energy is seen to decrease monotonically and uniformly in the downstream direction over the whole pipe cross section. This trend is intensified in the case of a higher rotational speed. In Fig. 7, the Reynolds stress is normalized in the same manner as in Fig. 6. As the flow proceeds downstream, the Reynolds stress in the vicinity of the wall is diminished with an increase in the rotation rate.

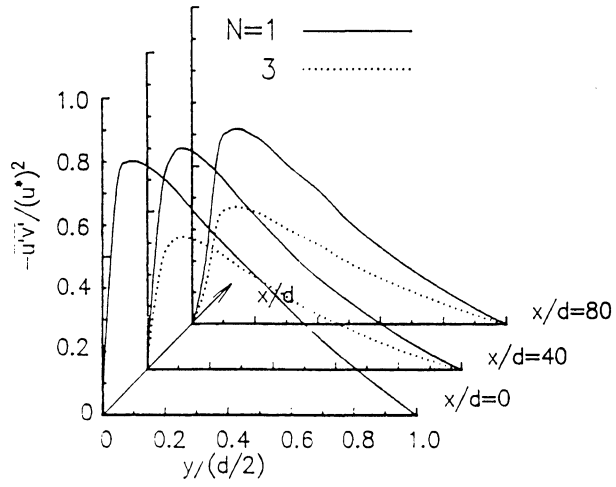

FIGURE 7 Streamwise variation of Reynolds stress profiles, using the k − ϵ model of Torii et al. [1990], for Re = 10,000.

In summary, a decrease in the Nusselt number and a suppression of the thermal development, as seen in Figs. 2, 3 and 4, is certainly caused by the axial rotation of the pipe. It is intensified with an increase in the rotation rate. The mechanism is that the axial rotation induces both a substantial deformation of the streamwise velocity profile and an attenuation in the turbulent kinetic energy and Reynolds stress along the flow, resulting in a deterioration of heat transfer performance and a suppression of the thermal development.

SUMMARY

Three different two-equation k-ϵ turbulence models have been employed to numerically investigate fluid flow and heat transfer in a slightly heated pipe rotating around its axis. Consideration is given to the influence of rotation rate on the velocity profile and flow structures in the thermally and hydrodynamically developing flow region. The results obtained are summarized as follows:

If the model function, C_3, is introduced into each of the ϵ equations, numerical results are in good agreement with experimental data in the existing literature. The local Nusselt number decreases monotonically in the downstream direction and approaches a constant value, and the axial rotation of the pipe suppresses thermal development and induces an attenuation in heat transfer performance. It is also disclosed that as the flow proceeds downstream, the streamwise velocity gradient near the wall is decreased and the turbulent kinetic energy and Reynolds stress are substantially reduced over the whole cross section. This tendency is amplified with an increase in the rotation speed. Consequently, the axial rotation of the pipe causes a substantial deformation of the streamwise velocity profiles and make the turbulent kinetic energy and Reynolds stress diminish. It results in both the deterioration of heat transfer performance and the suppression of thermal development in the entrance region of the pipe.

Nomenclature

C_μ, C_1, C_2	empirical constants of k-ϵ model
C_3	model function of k-ϵ model
d	pipe diameter, m
D	modification term in the wall region, in Eq. (10)
E	modification term in the wall region, in Eq. (11)
f_μ, f_1, f_2	model functions of k-ϵ model
h	heat transfer coefficient, W/Km^2

k	turbulent kinetic energy, m^2/s^2
N	rotation rate, W/U
Nu	Nusselt number, hd/λ
P	time-averaged pressure, Pa
Pr	Prandtl number
Pr_t	turbulent Prandtl number
q	heat flux, W/m^2
r	radial coordinate, m
Re	Reynolds number, Ud/ν
Ri	Richardoson number, Eq. (13)
R_t	turbulent Reynolds number, $k^2/\epsilon\nu$
R_τ	dimensionless distance in radial direction, y^+
$\overline{T}$	time-averaged temperature, K
t'	fluctuating temperature component, K
U	axial mean velocity over tube cross section, m/s
$\overline{u}$, $\overline{v}$, $\overline{w}$	time-averaged velocity components in axial, radial and tangential directions, respectively, m/s
$\overline{u}_{cp}$	axial velocity under the correction process, m/s
u', v', w'	fluctuating velocity components in axial, radial and tangential directions, respectively, m/s
u^*	friction velocity, m/s
W	tangential speed of rotating pipe wall, m/s
x	axial coordinate, m
y	distance from the wall, m
y^+	dimensionless distance, u^*y/ν
z^*	dimensionless length, x/(d/2)
α, α_t	molecular and turbulent thermal diffusivities, m^2/s
ϵ	turbulent energy dissipation rate, m^2/s^3
λ	molecular thermal conductivity, W/mK
ν, ν_t	molecular and turbulent viscosity, m^2/s
θ	coordinate in tangential direction
σ_k, σ_ϵ	turbulent Prandtl numbers for k and ϵ, respectively

Subscripts

in	inlet
w	wall
o	rotation

Superscripts

	time-averaged value
	fluctuation value

References

Bradshaw, P., 1969. The Analogy between Streamline Curvature and Buoyancy in Turbulent Shear Flow, *J. Fluid Mech.*, Vol. 36, pp. 177–191.

Hirai, S., Takagi, T., and Matumoto, M., 1986. Prediction of the Laminarization Phenomena in Turbulent Swirling Flows, *Trans, JSME* (in Japanese), Vol. 52, no. 476, pp. 1608–1616.

Kawamura, H., and Mishima, T., 1991. Numerical Prediction of Turbulent Swirling Flow in a Rotating Pipe by a Two-Equation Model of Turbulence (Fully Developed Swirling Flow), *Trans. JSME* (in Japanese), Vol. 57, no. 536, pp. 1251–1256.

Kikuyama, K., Murakami, M., Nishibori, K., and Maeda, K., 1983. Flow in an Axially Rotating Pipe (A Calculation of Flow in the Saturated region), *Bulletin of the JSME*, Vol. 26, no. 214, pp. 506–513.

Launder, B. E., and Sharma, B. I., 1974. Application of the Energy-Dissipation Model of Turbulence to the Calculation of Flow near a Spinning disk, *Letters in Heat and Mass Transfer*, no. 1, pp. 131–137.

Murakami, M., Kikuyama, K., 1980. Turbulent Flow in Axially Rotating Pipes, *Trans. ASME, J. Fluid Eng.*, Vol. 102, pp. 97–103.

Nagano, Y., Hishida, M., 1987. Improved Form of the k-ϵ Model for Wall Turbulent Shear Flows, *Trans. ASME*, Ser. D, Vol. 109, pp. 156–160.

Nishibori, K., Kikuyama, K., and Murakami, M., 1987. Laminarization of Turbulent Flow in the Inlet Region of an Axially Rotating Pipe, *JSME Int. J.*, Vol. 30, no. 260, pp. 255–262.

Patankar, S. V., 1980. *Numerical Heat Transfer and Fluid Flow*, Hemisphere, Washington, DC.

Reichi, G., and Beer, H., 1990. Fluid Flow and Heat Transfer in an Axially Rotating Pipe, in *Dynamics of Rotating Machinery*, Eds. J. H. Kim and W. J. Yang, pp. 273–288, Hemisphere, Washington, DC.

Rodi, W., Examples of Turbulence Models for Incompressible Flows, *AIAA, J.*, Vol. 20, pp. 872–879.

Torii, S., Shimizu, A., Hasegawa, S., and Higasa, M., 1990. Laminarization of Strongly Heated Gas Flow in a Circular Tube (Numerical Analysis by Means of a Modified k-ϵ Model), *JSME Int. J.*, Ser. II, Vol. 33, no. 3, pp. 538–547.

Torii, S., and Yang, W. J., 1995. Numerical Prediction of Fully Developed Turbulent Swirling Flows in an Axially Rotating Pipe by Means of a Modified k-ϵ Turbulence Model, *Int. J. Numerical Methods for Heat & Fluid Flow*, Vol. 5, pp. 175-183

Weigand, B., and Beer, H., 1992. Fluid Flow and Heat Transfer in an Axially Rotating Pipe: The Rotational Entrance, in *Rotating Machinery*, Eds. J. H. Kim and W. J. Yang, pp. 325–340, Hemisphere, Washington, DC.

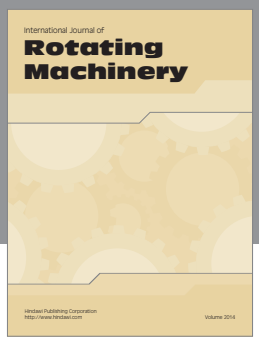

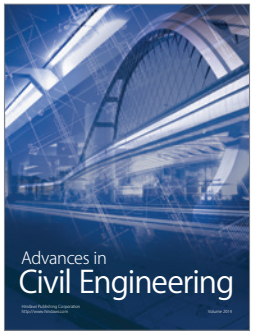

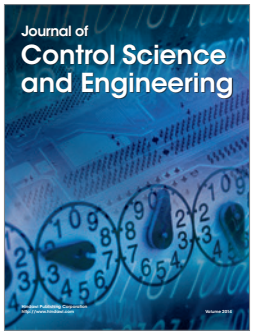

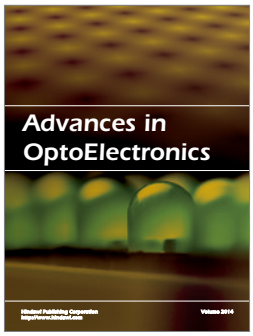

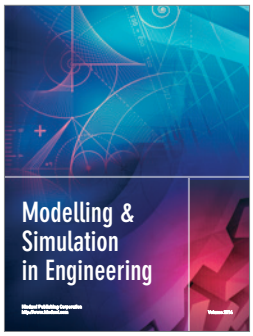

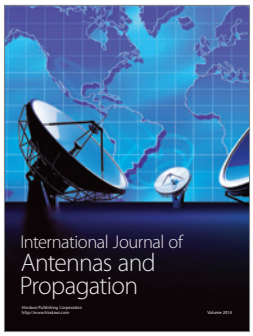

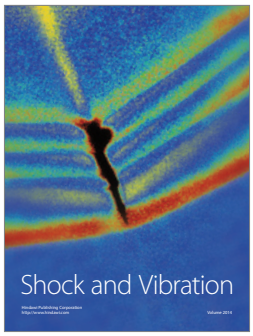

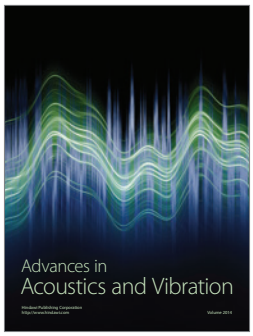

Hindawi

Submit your manuscripts at
http://www.hindawi.com